THE JOURNAL OF PHYSICAL CHEMISTRY Letters

Letter

pubs.acs.org/JPCL

Terms of Use

Fingerprints of Adiabatic versus Diabatic Vibronic Dynamics in the Asymmetry of Photoelectron Momentum Distributions

Mirjam Falge,[†] Volker Engel,[†] and Stefanie Gräfe*[,‡]

[†]Institut für Physikalische und Theoretische Chemie, Universität Würzburg, Hubland Campus Nord, Emil-Fischer-Strasse 42, 97074 Würzburg, Germany

[‡]Institute for Theoretical Physics, Vienna University of Technology, Wiedner Hauptstrasse 8-10, A-1040 Vienna, Austria

ABSTRACT: When the Born−Oppenheimer approximation is valid, electrons adiabatically follow the nuclear motion in molecules. For strong nonadiabatic coupling between electronic states, one encounters a diabatic motion where the electrons remain local and do not adapt to molecular geometry changes. We show that the mentioned limiting cases are reflected differently in the asymmetry of time-resolved photoelectron momentum distributions. Whereas for adiabatic dynamics, the asymmetry directly maps the time-dependent average nuclear momentum, in the diabatic case, the asymmetry is determined by a nonclassical interference effect arising from the mixing of wave function components in different electronic states, which is present at times nonadiabatic transitions take place.

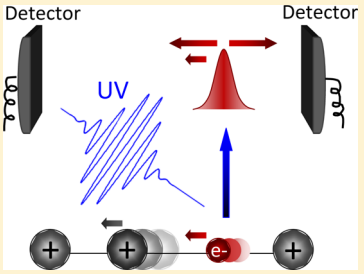

SECTION: Spectroscopy, Photochemistry, and Excited States

The Born−Oppenheimer (BO) separation of electronic and nuclear motion,[1] leading to the concept of potential energy surfaces, is one of the most important approximations to understand, e.g., the course of a chemical reaction or the vibronic structure of UV−vis absorption spectra. Within the BO approach, the electrons *adiabatically* follow geometry changes in molecules. Mathematically, the BO approximation works well when the derivatives of the electronic wave function with respect to the nuclear coordinates are small. Often, however, the BO approximation fails, which is the case when potential energy curves of energetically close lying electronic states show an avoided crossing,[2,3] or, in the more general case, the potential surfaces exhibit conical intersections.[4−6] In such regions of nuclear coordinate space, the character of the electronic wave functions changes abruptly, giving rise to large if not divergent couplings between the electronic states.[7] In such situations, it is favorable to adopt another approach where such divergences do not occur. The electronic states that minimize the above-mentioned couplings are called *diabatic* states.[8,9] In the diabatic picture, the electronic wave functions remain localized and exhibit only minor (and ideally no) changes if a region of nonadiabatic interaction is passed.

Below, we identify signatures of adiabatic and diabatic dynamics without relying on the separation of electronic and nuclear motion, i.e., by solving the time-dependent Schrödinger equation for the coupled vibronic dynamics. Due to the large computational cost, this is only possible within descriptions of reduced dimensionality. We therefore adopt a model that involves a single electron (coordinate x) and a nucleus (coordinate R), moving in one dimension between two fixed nuclei.[10,11] The electron-nuclei interactions are parametrized with error-functions (erf) involving screening parameters, and the potential energy is (in atomic units)

$$V(x,R) = \frac{Z^2}{|L/2-R|} + \frac{Z^2}{|L/2+R|} - \frac{Z\,\mathrm{erf}(|L/2-x|/R_f)}{|L/2-x|} - \frac{Z\,\mathrm{erf}(|R-x|/R_c)}{|R-x|} - \frac{Z\,\mathrm{erf}(|L/2+x|/R_f)}{|L/2+x|} \quad (1)$$

Our computations use a charge number of $Z = 1$ for all nuclei and a screening parameter of R_f =1.5 Å. The fixed ions are located at $R = \pm L/2$ with L = 10 Å. The beauty of the model is that, upon adjusting the remaining parameter R_c, one is able to switch from a situation of an adiabatic to a diabatic motion.[12,13] As an observable, we regard the time-dependent photoelectron momentum (p) distribution $\sigma(p,T)$[14−16] obtained from ionization with a laser pulse interacting at different times T. Separating the electrons that are emitted with positive/negative momenta leads to spectra $\sigma^{\pm}(p,T)$, respectively. Integration over p then yields the spectrum $\sigma^{\pm}(T)$ which enters into the definition of the (normalized) asymmetry as

$$A(T) = \frac{\sigma^{+}(T) - \sigma^{-}(T)}{\sigma^{+}(T) + \sigma^{-}(T)} \quad (2)$$

Such asymmetries have recently been investigated experimentally[17−19] and theoretically.[20−24] We calculate $A(T)$ from the wave function $\psi(x, R, t, T)$, which is obtained by numerically solving the time-dependent Schrödinger equation.[25] Briefly, after

Received: July 19, 2012
Accepted: August 27, 2012
Published: August 27, 2012

   dx.doi.org/10.1021/jz3009826 | J. Phys. Chem. Lett. 2012, 3, 2617−2620

the pulse interaction, the wave function that has reached the asymptotic region of large electron coordinate ($|x| > 100$ Å in our calculation) is transformed to electronic momentum space ($\psi_{as}(p, R, t, T)$), and $S^{\pm}(p, T)$ is calculated as

$$S^{\pm}(p, T) = \lim_{t\to\infty} \int dR\, |\psi_{as}(p, R, t, T)|^2 \quad (3)$$

by integration over the nuclear coordinate R; for details, see ref 26.

To characterize the system, we first calculate the adiabatic potentials $V_n(R)$ and corresponding electronic wave functions $\varphi_n(x, R)$ by imaginary time-propagation.[27] The potentials for the two lowest electronic states ($n = 0,1$) are shown in Figure 1. The

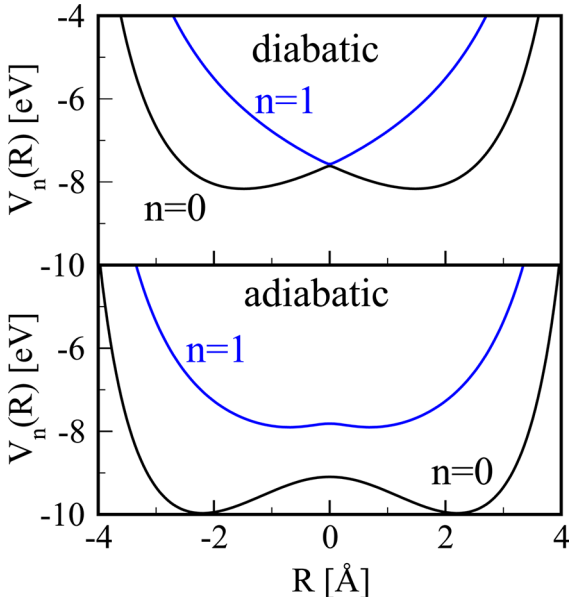

Figure 1. Potential curves suggesting an *adiabatic* motion in the electronic ground state and for the case when a strong coupling between the ground and first excited state is present (*diabatic*).

two curves in the lower panel ($R_c = 1.5$ Å) are well separated in energy, suggesting that a nuclear motion in the electronic ground state is described accurately within the BO approximation, i.e., the coupling to other electronic states can be neglected. On the other hand, the curves obtained for a screening parameter of $R_c = 2.5$ Å exhibit an avoided crossing at the configuration with $R = 0$, suggesting a strong nonadiabatic coupling. The two situations will be referred to as adiabatic and diabatic, respectively, in what follows. Note that the potential energy curves in Figure 1 are only used for the purpose of interpretation; as we solve the full-coupled system, all electronic (and vibrational) eigenstates are implicitly contained in the dynamics.

In Figure 2 we show the dynamics of the electronic and nuclear densities defined as

$$\rho(x, t) = \int dR\, |\psi(x, R, t)|^2 \quad (4)$$

$$\rho(R, t) = \int dx\, |\psi(x, R, t)|^2 \quad (5)$$

where $\psi(x, R, t)$ is the time-dependent wave function of the unperturbed system. For the adiabatic case (left panels), the wave function at time $t = 0$ is taken as $\psi(x, R, 0) = e^{-\beta(R-R_0)^2}\varphi_0(x, R)$, with $\beta = 7.14$ Å and $R_0 = -0.9$ Å. Thus, we start in the electronic ground state. The nuclear density shows a localized wave packet

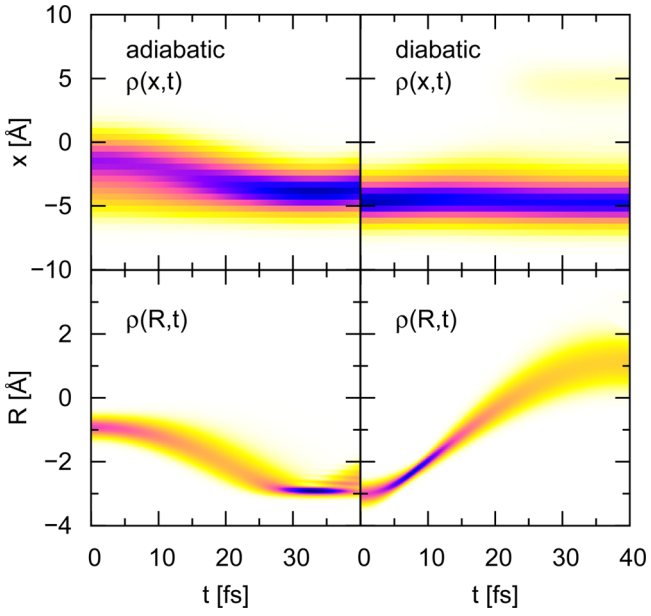

Figure 2. Time-dependent electronic (upper panels) and nuclear (lower panels) densities are displayed for the case of adiabatic and diabatic motion, as indicated.

motion. Regarding the ground state potential (Figure 1), it is seen that, due to the initial condition, the motion is restricted to take place in the left-hand well of the potential, which means that we encounter an adiabatic motion in a single electronic state. This is confirmed by inspection of the population in the ground state, which remains constant during the time-interval considered (Figure 3, lower left panel). The electronic density

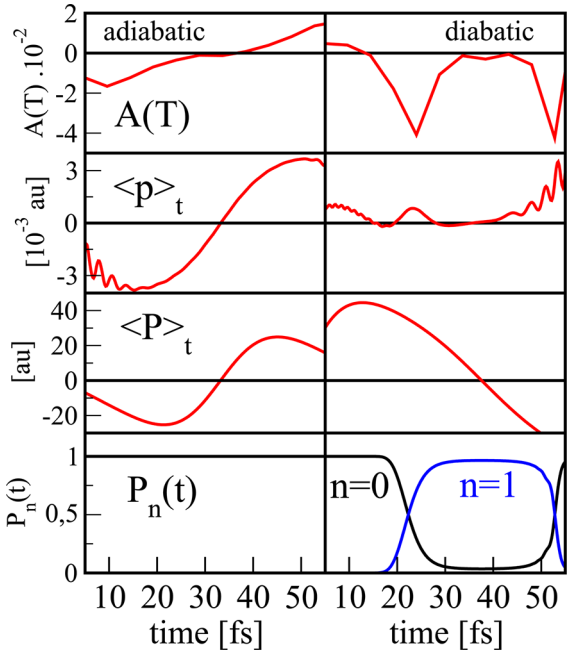

Figure 3. Time-dependence of the populations $P_n(t)$ in the electronic states ($n = 0,1$), the expectation values of the nuclear momentum $\langle P\rangle_t$ and electron momentum $\langle p\rangle_t$ and the asymmetry $A(T)$ are displayed for the case of the adiabatic and diabatic motion, as indicated.

(upper left panel of Figure 2) follows the nuclear density as is expected from adiabatic dynamics.

dx.doi.org/10.1021/jz3009826 | J. Phys. Chem. Lett. 2012, 3, 2617−2620

Next, we regard the diabatic dynamics. There, the time-dependence of the nuclear density (starting with a Gaussian nuclear wave packet at $R_0 = -3.0$ Å) resembles the one in the adiabatic case with the difference that here the initial condition is chosen such that the motion extends into regions of positive values of R. The population analysis shows that, upon passing the symmetric configuration ($R = 0$), the population is transferred from the ground state to the first excited state almost completely (Figure 3, lower right panel). This suggests a dynamics on a diabatic potential, which, for negative values of R, consists of the branch of the adiabatic potential $V_0(R)$ and, for positive R, is the potential $V_1(R)$. Then, by definition, the electronic density should not change essentially during the dynamics and remain localized. This, indeed, is seen in the time-dependent electron density $\rho(x,t)$, which is shown in Figure 2, right upper panel.

At this point, the question arises whether the character of the quantum dynamics, being adiabatic or diabatic, is reflected in an observable. Therefore, we suggest regarding the time-resolved photoelectron asymmetry $A(T)$, as defined above. Before details of the numerical calculation are presented, let us speculate on what to expect intuitively in the cases of adiabatic and diabatic motion. In the former case, the adiabatic motion of the electron, being attached to the moving nucleus, results in an electron momentum expectation value $\langle p \rangle_t$, which is positive/negative if the nucleus moves in the positive/negative direction of R, respectively. Then, upon ionization, electrons are emitted preferentially in the direction determined by the mean momentum in the initial state. From this classical consideration, it is then anticipated that ionization produces electron distributions with an asymmetry determined by the nuclear motion, and thus $A(T)$ should reflect its direction. That this expectation indeed is correct is documented in Figure 3 (left panels), which compares the expectation values of the nuclear and electronic momentum with the asymmetry. In the numerical calculation we use an ionizing XUV-pulse with a wavelength of 62 nm, an intensity of 10^{13} W/cm^2, and a width of the Gaussian envelope function of 4 fs. The times $t = T$ refer to the maximum of the pulse envelope-function.

For the diabatic dynamics, a rather different behavior is anticipated. Because the electronic density remains localized and, to a first approximation, does not change during the nuclear wave packet dynamics, the average electron momentum is zero, and only minor changes in the asymmetry are expected. Figure 3 (right-hand panels) shows that the electron momentum indeed remains small if compared to the adiabatic case besides the fact that the nuclear momentum assumes similar positive and negative values. The asymmetry does not exhibit sign changes upon a change in the direction of the nuclear motion and thus does not reflect the latter. It is small for times when the nuclear density is not located close to the region of the avoided crossing. However, it assumes larger values during the time the nonadiabatic transition occurs.

To gain some insight into the origin of this behavior, we calculate the asymmetry employing first-order time-dependent perturbation theory. Expanding the initial state in terms of the adiabatic electronic eigenfunctions (in the electronic momentum representation) of the two electronic states that participate, the wave function describing the detachment is of the form

$$\psi^+(p, R, t, T) = \sum_{n=0}^{1} \hat{B}_T \psi_n^a(R, t)\varphi_n(p, R) = \psi_0^+(p, R, t, T) + \psi_1^+(p, R, t, T), \quad (6)$$

where we explicitely noted the time-dependence of the moving wave packets. The operator $\hat{B}_T$ maps, to first order, the initial state onto the final state in the detachment continuum. The photoelectron spectrum, and thus the asymmetry, then consists of three terms representing detachment out of the ground state, out of the excited state, and an interference contribution:

$$\sigma(p, T) = \lim_{t\to\infty} \int dR\, [|\psi_0^+(p, R, t, T)|^2 + |\psi_1^+(p, R, t, T)|^2 + 2\mathcal{R}((\psi_0^+(p, R, t, T))^* \psi_1^+(p, R, t, T))] \quad (7)$$

In Figure 4, we show the asymmetry and its decomposition. The figure shows that the interference term contributes most

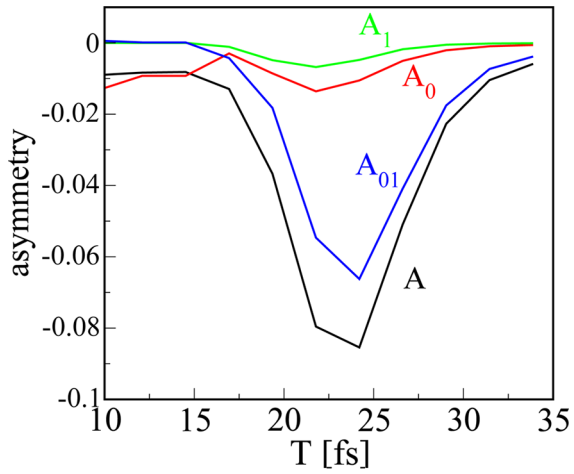

Figure 4. Time-dependent asymmetry $A(T)$ and its decomposition into a contribution resulting from the initial electronic ground state ($A_0(T)$), the excited state ($A_1(T)$), and the interference term $A_{01}(T)$.

significantly to the asymmetry. Let us therefore discuss this term ($\sigma_{01}(p, T)$) and, for simplicity, regard the most significant contribution to the spectrum originating from the fixed nuclear distance $R = R_T$ where the nuclear density has its maximum at time T. Then, one obtains

$$\sigma_{01}(p, R_T) = 2\mathcal{R}((\psi_0^a(R_T))^* \psi_1^a(R_T)(\hat{B}_T\varphi_0(p, R_T))^* \hat{B}_T\varphi_1(p, R_T)) \quad (8)$$

Because we discuss a diabatic nuclear motion, it is more appropriate to replace the adiabatic components of the two-state nuclear wave function by the diabatic ones using the transformation

$$\begin{pmatrix} \psi_0^a(R_T) \\ \psi_1^a(R_T) \end{pmatrix} = \begin{pmatrix} \cos\Theta_T & \sin\Theta_T \\ -\sin\Theta_T & \cos\Theta_T \end{pmatrix} \begin{pmatrix} \psi_0^d(R_T) \\ \psi_1^d(R_T) \end{pmatrix} \quad (9)$$

where $\Theta_T = \Theta(R_T)$ is the so-called *mixing angle* depending on the nuclear coordinate.[7,28] This angle is zero at distances smaller than the coupling region and $\pi/2$ for distances larger than the coupling region. In our case, where the wave packet dynamics takes place (almost) exclusively in the diabatic state with $n = 0$, we have $\psi_1^d(R_T) = 0$, so that

$$\sigma_{01}(p, R_T) = -2\cos\Theta_T \sin\Theta_T |\psi_0^d(R_T)|^2 \times \mathcal{R}[(\hat{B}_T\varphi_0(p, R_T))^* (\hat{B}_T\varphi_1(p, R_T))] \quad (10)$$

dx.doi.org/10.1021/jz3009826 | J. Phys. Chem. Lett. 2012, 3, 2617−2620

Here we encounter a modulation of the spectrum with the function $(-\cos \Theta_T \sin \Theta_T)$. The same then applies to the asymmetry, and thus the particular time-dependence of the latter during the nonadiabatic transition, which is seen in Figure 3, can be rationalized.

To conclude, we have shown that for a BO adiabatic motion, the photoelectron momentum asymmetry directly correlates with the direction of the vibrational motion, information that is difficult to extract from other time-resolved photoionization signals. On the other hand, for a strong nonadiabatic coupling, the asymmetry maps the population transfer dynamics between the involved electronic states, which correlates with the mixing of the components of the wave packet in these states. Although a rather simple model is employed in the present study, we believe that the findings can be generalized to situations involving several electrons and nuclei. The concepts of adiabatic and diabatic nuclear motion is not restricted to the motion involving a single nuclear degree-of-freedom. Rather, it occurs also in geometry changes involving all of the nuclei bound in a molecule.[4−9] We expect the dynamics in multidimensional systems to induce an asymmetry in the photoelectron distribution as well, which might, however, be more easily visualized in channel-resolved photoelectron angular distributions.[29] Work along these lines is in progress.

AUTHOR INFORMATION

Corresponding Author

*E-mail: stefanie.graefe@tuwien.ac.at.

Notes

The authors declare no competing financial interest.

ACKNOWLEDGMENTS

M.F. acknowledges financial support by the State of Bavaria (Bayerisches Eliteförderungsgesetz). S.G. acknowledges financial support by the Austrian Science Fund FWF, project number V193-N16. This work was supported by the travel grant of the International Office of the Vienna University of Technology.

REFERENCES

(1) Born, M.; Huang, K. *Theory of Crystal Lattices*; Oxford University Press: London, 1954.

(2) von Neumann, J.; Wigner, E. On the Behavior of Eigenvalues in Adiabatic Processes. *Phys. Z.* **1929**, *30*, 467.

(3) Teller, E. The Crossing of Potential Surfaces. *J. Phys. Chem.* **1937**, *41*, 109−116.

(4) Yarkony, D. R. Diabolical Conical Intersections. *Rev. Mod. Phys.* **1996**, *68*, 985−1013.

(5) Domcke, W., Yarkony, D. R., Köppel, H., Eds. *Conical Intersections: Theory, Computation and Experiment*; World Scientific: Singapore, 2011.

(6) Domcke, W.; Yarkony, D. R. Role of Conical Intersections in Molecular Spectroscopy and Photoinduced Chemical Dynamics. *Annu. Rev. Phys. Chem.* **2012**, *63*, 325−352.

(7) Domcke, W.; Stock, G. Theory of Ultrafast Nonadiabatic Excited-State Processes and Their Spectroscopic Detection in Real Time. *Adv. Chem. Phys.* **1997**, *100*, 1.

(8) Sidis, V. Diabatic Potential Energy Surfaces for Charge-Transfer Processes. *Adv. Chem. Phys.* **1992**, *82*, 73.

(9) Pacher, T.; Cederbaum, L.; Köppel, H. Adiabatic and Quasiadiabatic States in a Gauge Theoretical Framework. *Adv. Chem. Phys.* **1993**, *84*, 293.

(10) Shin, S.; Metiu, H. Nonadiabatic Effects on the Charge Transfer Rate Constant: A Numerical Study of a Simple Model System. *J. Chem. Phys.* **1995**, *102*, 9285−9295.

(11) Shin, S.; Metiu, H. Multiple Time Scale Quantum Wavepacket Propagation: Electron-Nuclear Dynamics. *J. Phys. Chem.* **1996**, *100*, 7867−7872.

(12) Erdmann, M.; Marquetand, P.; Engel, V. Combined Electronic and Nuclear Dynamics in a Simple Model System. *J. Chem. Phys.* **2003**, *119*, 672−679.

(13) Erdmann, M.; Baumann, S.; Gräfe, S.; Engel, V. Electronic Predissociation: A Model Study. *Eur. Phys. J. D* **2004**, *30*, 327−333.

(14) Stolow, A. Femtosecond Time-Resolved Photoelectron Spectroscopy of Polyatomic Molecules. *Annu. Rev. Phys. Chem.* **2003**, *54*, 89−119.

(15) Stolow, A.; Bragg, A. E.; Neumark, D. M. Femtosecond Time-Resolved Photoelectron Spectroscopy. *Chem. Rev.* **2004**, *104*, 1719−1757.

(16) Wollenhaupt, M.; Engel, V.; Baumert, T. Femtosecond Laser Photoelectron Spectroscopy on Atoms and Small Molecules: Prototype Studies in Quantum Control. *Annu. Rev. Phys. Chem.* **2005**, *56*, 25−56.

(17) Kienberger, R.; et al. Atomic Transient Recorder. *Nature* **2004**, *427*, 817−821.

(18) Dowek, D.; Pérez-Torres, J. F.; Picard, Y. J.; Billaud, P.; Elkharrat, C.; Houver, J. C.; Sanz-Vicario, J. L.; Martín, F. Circular Dichroism in Photoionization of H_2. *Phys. Rev. Lett.* **2010**, *104*, 233003-1−233003-4.

(19) Kling, M. F.; et al. Control of Electron Localization in Molecular Dissociation. *Science* **2006**, *312*, 246−248.

(20) Chelkowski, S.; Bandrauk, A. D.; Apolonski, A. Phase-Dependent Asymmetries in Strong-Field Photoionization by Few-Cycle Laser Pulses. *Phys. Rev. A* **2004**, *70*, 013815-1−013815-9.

(21) Perez-Torres, J. F.; Morales, F.; Sanz-Vicario, J. L.; Martín, F. Asymmetric Electron Angular Distributions in Resonant Dissociative Photoionization of H_2 with Ultrashort XUV Pulses. *Phys. Rev. A* **2009**, *80*, 011402-1−011402-4.

(22) Bandrauk, A. D.; Chelkowski, S.; Corkum, P. B.; Manz, J.; Yudin, G. L. Attosecond Photoionization of a Coherent Superposition of Bound and Dissociative Molecular States: Effect of Nuclear Motion. *J. Phys. B: At. Mol. Opt. Phys.* **2009**, *42*, 134001-1−134001-7.

(23) Arasaki, Y.; Wang, K.; McKoy, V.; Takatsuka, K. Monitoring the Effect of a Control Pulse on a Conical Intersection by Time-Resolved Photoelectron Spectroscopy. *Phys. Chem. Chem. Phys.* **2011**, *13*, 8681−8689.

(24) Gräfe, S.; Engel, V.; Ivanov, M. Yu. Attosecond Photoelectron Spectroscopy of Electron Tunneling in a Dissociating Hydrogen Molecular Ion. *Phys. Rev. Lett.* **2008**, *101*, 103001-1−103001-4.

(25) Feit, M. D.; Fleck, J. A.; Steiger, A. Solution of the Schrödinger Equation by a Spectral Method. *J. Comput. Phys.* **1982**, *47*, 412−433.

(26) Falge, M.; Engel, V.; Gräfe, S. Time-Resolved Photoelectron Spectroscopy of Coupled Electron-Nuclear Motion. *J. Chem. Phys.* **2011**, *134*, 184307−1−184307−8.

(27) Kosloff, R.; Tal-Ezer, H. A Direct Relaxation Method for Calculating Eigenfunctions and Eigenvalues of the Schrödinger Equation on a Grid. *Chem. Phys. Lett.* **1986**, *127*, 223−230.

(28) Köppel, H.; Gronki, J.; Mahapatra, S. Construction Scheme for Regularized Diabatic States. *J. Chem. Phys.* **2001**, *115*, 2377−2388.

(29) Seideman, T. Time-Resolved Photoelectron Angular Distributions: Concepts, Applications, and Directions. *Annu. Rev. Phys. Chem.* **2002**, *53*, 41−65.